METHODS FOR ANALYZING DEFORMATION OF *IN VITRO* TISSUE MODELS DURING SIMULATED ACUPUNCTURE THERAPY

by

LOWELL TAYLOR EDGAR

A Dissertation submitted to the

Graduate School-New Brunswick

Rutgers, The State University of New Jersey

The Graduate School of Biomedical Sciences

and

University of Medicine and Dentistry of New Jersey

in partial fulfillment of the requirements

for the degree of

Master of Science

Graduate Program in Graduate Program in Biomedical Engineering

written under the direction of

Dr. David Shreiber

and approved by

_____

_____

_____

_____

New Brunswick, New Jersey

[October 2009]

ABSTRACT OF THE THESIS

METHODS FOR ANALYZING DEFORMATION OF *IN VITRO* TISSUE MODELS

DURING

SIMULATED ACUPUNCTURE THERAPY

By LOWELL TAYLOR EDGAR

Thesis Director:

Dr. David Shreiber

Traditional acupuncture therapy involves insertion and manipulation of fine needles through the skin at various points of the body. Studying acupuncture therapy both *in vivo* and *ex vivo* has revealed that during needle manipulation, loose connective tissue under the skin couples and winds to the needle, producing profound deformation that could act as a mechanism for the treatment's therapeutic benefits. In order to study this biophysical phenomenon in a controlled setting, we have constructed a simplified model of acupuncture therapy *in vitro*. We believe that using connective tissue models in our assay allows unique observations not permitted in previous investigations of acupuncture therapy. Two specific goals of our *in vitro* assay of acupuncture therapy are: 1) Quantitatively measure the relationship between tissue parameters and the ability to respond to acupuncture therapy, and 2) Make direct observations of deformation invoked by needle manipulation. The objective of this thesis was to construct quantitative tools that allow us to perform these desired observations. We utilize various microscopy and images processing tools to extract quantitative data from our system, including polarized light microscopy (PLM) to assess aligning extracellular matrix fibers in deforming tissue and automated tracking of displacing beads suspended within our tissue models to characterize the deformation during simulated acupuncture therapy. Our system and the

tools developed for this thesis demonstrate accuracy by corroborating with previously published research and precision by producing reliable, consistent results. These tools have allowed us to make several observations of the biophysical behavior of tissue during acupuncture therapy and the role of mechanostructural properties in the tissue's ability to respond to needle manipulation. In conjunction with *in vivo* and *ex vivo* research endeavors, we believe that our *in vitro* tools provide valuable insight towards investigating the role of tissue deformation as a mechanism for acupuncture therapy.

I would like to acknowledge the following people and express my gratitude for their contribution towards our research goals:

Dr. David Shreiber

Dr. Helen Buettner

Dr. Troy Shinbrot

Dr. Anant Madabhushi

Dr. Peng Song

Margaret Julias

Alice Seneres

Satish Viswanath

Table of Contents

List of Figures

I. Introduction

Acupuncture is an ancient Chinese medical practice that involves the insertion of fine needles into various points on the body, termed 'acupuncture points.' According to tradition, acupuncture points are specific locations where the *meridians*, or pathways for the flow of the life-force *qi,* can be accessed. States of disease and disorder occur due to a blockage of the flow of qi, resulting in an imbalance between *yin* and *yang.* Proper flow can be restored by accessing the meridians at these points by acupuncture therapy, hence restoring the flow of qi and returning the body to its healthy balanced state. Today acupuncture therapy is accepted in the treatment of several ailments including pain, nausea, and allergies[1]. Despite its many potential clinical uses, the mechanism as to how acupuncture therapy produces its results is still largely unknown.

During acupuncture therapy, needles are inserted into the patient's epidermis, down through adipose and subcutaneous connective tissue, and into the underlying muscle layer. The inserted needle is then manually manipulated by the acupuncture therapist, typically by needle rotation and/or pistoning, producing a phenomenon known as *de qi*. De qi is perceived by the patient as a heaviness surrounding the needle, and experienced by the therapist as an increased resistance to further manipulation known as needle grasp. While studying acupuncture *in vivo*, Langevin et al suggested that needle grasp may be explained by the coupling and winding of collagen fibers in the subcutaneous connective tissue above the muscle around the needle as it is rotated[2-5]. Acupuncture points and meridians have been found to correlate anatomically with thick regions of loose connective tissue at intermuscular cleavage planes[8], and needling at acupuncture points produces more needle grasp than at control points[2]. Langevin hypothesized that the mechanical stresses imparted during acupuncture could provide signals to nearby cells, which ultimately may initiate some of the beneficial outcomes of acupuncture. Recent research findings support this notion and have forged a recent emphasis on connective tissue involvement in the mechanism of acupuncture therapy.

Acupuncture needling in rat tissue explants revealed distinct cytoskeletal changes in fibroblasts populating loose connective tissue[6, 7]. These *ex vivo* observations suggest that the extreme deformation invoked by acupuncture therapy in the connective tissue produces strong mechanical signals across cell membranes. Mechanotransduction stimulation of local fibroblasts could therefore play a significant role in the mechanism of acupuncture therapy[5-7].

This recent emphasis on connective tissue involvement during acupuncture therapy raises questions about the properties of this tissue that allow this unique response to acupuncture needling. Studying the mechanism of fiber winding is difficult in both *in vivo* and *ex vivo* assays as previously described due to the inherent biological variability of tissue and limited access by measurement tools. Hence, in order to investigate the tissue-level mechanism of needle rotation and fiber winding as it relates to acupuncture therapy, we have designed an *in vitro* assay which will allow us to study the tissue response to needling in a simplified, controlled setting. Using this system, we can analyze the phenomenon of fiber winding and the role of matrix properties on this behavior, tasks that would prove quite difficult *in vivo*.

Using our *in vitro* assay of acupuncture, we can investigate the role of connective tissue in acupuncture therapy from a unique approach. Fibrous protein such as collagen represents the most significant structural element in the extracellular matrix, and it is hypothesized that these proteins are responsible for the biophysical response of connective tissue during acupuncture therapy. For these reasons, we have chosen to investigate the behavior of fibrous protein to acupuncture needle rotation, with the following major goals in mind:

Objective 1 – Assess the degree of fiber winding across various conditions to determine the effect of fibrous protein matrix properties on tissue response.

Objective 2 – Directly observe the biophysical response of fibrous protein networks during simulated acupuncture therapy.

In order to perform our analysis as desired, quantitative tools need to be developed for our *in vitro* system. We simulate acupuncture therapy by inserting a needle through a gel and rotating using a computer-controlled motor. During needle rotation we observe the resulting fiber winding using microscopy, and by utilizing various imaging tools we can proceed to extract quantitative data that represents the behavior of the system given the conditions. Polarized light microscopy (PLM) is one such technique we can use to study fiber alignment in the fibrous protein matrix as the deformation caused by needle rotation progresses. PLM allows for the extraction of a quantitative index (magnitude and/or rate of fiber alignment) that can be compared across different matrix properties in order to assess the effects of these properties on fiber winding and tissue response (see Section II). Another useful quantitative tool we can utilize in our *in vitro* assay is the use of fiduciary markers of motion, such as polystyrene beads seeded within a fibrous protein gel, in order to directly measure tissue displacement induced by acupuncture needle rotation (see Section III).

The goal of this thesis is to develop the algorithms that will allow us to take raw data, perform the necessary image processing, and execute computational routines to extract relevant quantitative data. A primary requirement for these algorithms is the ability to determine the differences in biophysical behavior across gel conditions in a reliable fashion. Once these tools are available, we can use our *in vitro* assay to study the mechanism of fiber winding and its role in the mechanism of connective tissue involvement in acupuncture therapy on a basic level. This analysis will in turn provide important biophysical observations for the continuing exploration of the role of mechanotransduction in acupuncture therapy.

II. Objective 1 – Assess the degree of fiber winding across various conditions to determine the effect of fibrous protein matrix properties on tissue response.

IIA. Introduction

Polarized light microscopy (PLM) is a valuable tool for analyzing isotropy in materials and has been previously used to describe the orientation of fibers in biological tissues[9]. Incorporating PLM into our *in vitro* assay of acupuncture allows us to document the effect of properties within the connective tissue on fiber winding, perhaps explaining what properties allow this tissue to exhibit its unique response to needle manipulation.

When light travels through a polarizer, it constrains the oscillations of electromagnetic waves to a single planar orientation determined by the polarization axis. PLM imaging, in its simplest application, involves positioning a material between 'cross-polars,' or polarizers at 90° apart. Light traveling through this filter configuration will not be transmitted since the two polarization axes are orthogonal. If a material with anisotropy is imaged between cross-polars, such as a fibrillar matrix with fibers aligned a certain axis, the material can change the orientation of light waves allowing light to travel through the optic train. When inducing fiber alignment in a collagen gel by acupuncture needling, the darkest areas in PLM images correlate to fibers oriented parallel or perpendicular to either polarization axis, while bright areas in the images occur where collagen fibers orient 45° to the optical axes.

We select type I collagen gels as our proof-of-principle model being that collagen is major protein component in loose connective tissue. As described in [10], fibers in the collagen gel prior to needling are randomly oriented and allow little to no light transmission in the PLM configuration. Once needling begins, fibers align circumferentially immediately around the needle and then transitionally to radially aligned in away from the needle. The intensity of transmitted light through the optic train depends on the angle of fiber alignment relative to the axes of polarization, with minimum intensity produced by fibers oriented along either of the two orthogonal polarization axes. This leads to the characteristic '4-leaf clover' birefringence pattern that appears in the

images (Fig. 1). This bright area corresponding to aligned fibers increases in size as the needling progresses, which we correlate to an increase in the amount of aligned fibers in the collagen network, indicating increasing deformation. The area of aligned fibers produced by acupuncture needling can be extracted via use of an image processing algorithm and can be used to compare the degree of fiber alignment across various parameter changes in the collagen matrix.

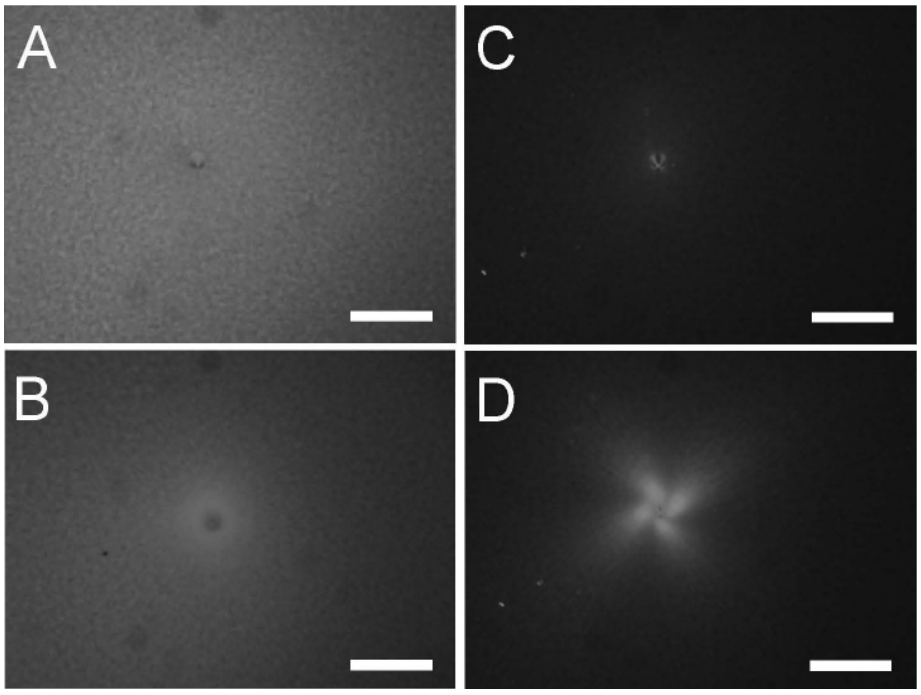

Figure 1 – 2.0 mg/mL Type I collagen gel imaged before and after 2 needle rotations. Brightfield imaging of collagen prior to needle rotation (A) and after need rotation (B) show an increase in fiber density around the needle as a result of fiber winding. Polarized light imaging reduces the signal in collagen gels to aligned fibers. Prior to needle rotation (C), only needle is observed. After needle rotation induces fiber winding (D) the aligned fibers change the orientation of incoming polarized light, resulting in the characteristic '4-leaf clover' birefringence pattern. Bar 1mm.

IIB. Methods

i. Collagen Gel Preparation

All collagen gels were prepared as described in [9]. Collagen gels were prepared at various collagen concentrations diluting various volumes of a stock solution of 3.75 mg/mL lyophilized collagen dissolved in 0.02 N acetic acid. Stock solution was neutralized to physiologic pH (7.2-7.4) with 0.1 N NaOH and further diluted with M199 and 10x MEM media. The final collagen solution was then poured into a glass-bottom MatTek dish and incubated at 37° for four hours to ensure complete fibril formation.

ii. Polarized Light Imaging

Our *in vitro* assay of collagen fiber alignment using polarized light microscopy (PLM) is described in Fig. 2. The collagen sample was situated between cross-polars, and images were captured using a dissection microscopy clamped under the sample to capture light transmitted through the optic train. A computer-controlled motor was used to simulate acupuncture therapy by rotating a stainless steel needle. The needle was inserted into the gel at a depth of 3 mm and rotated for 10 revolutions at a speed of 0.3 rev/second. A fiber-optic ring light was attached to the motor to provide a light source, and images were captured using a USB CCD camera at 6 frames per second.

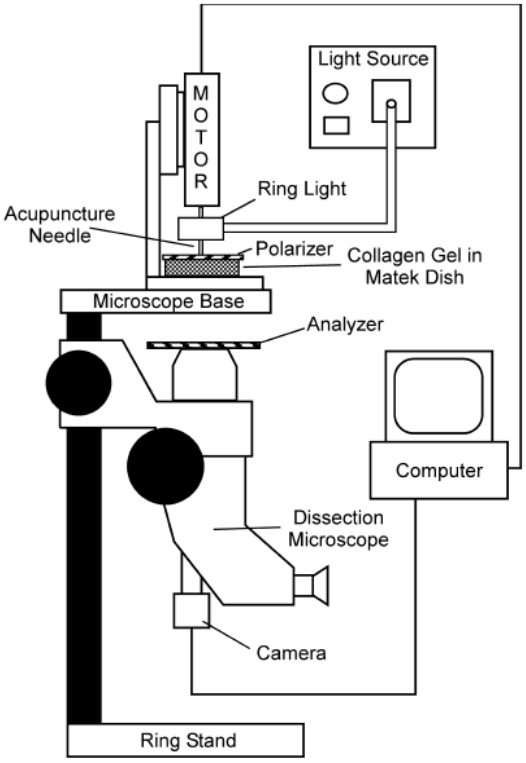

Figure 2 – Schematic of our *in vitro* assay of acupuncture therapy. The sample is placed in between cross-polars and needle using a computer-controlled motor. Aligned fibers allow the light emanating from the fiber optic light source to pass through the analyzer. Transmitted light is captured by a mounted dissection microscope and a CCD camera.

iii. Image Processing

All captured PLM images were subjected to an image processing algorithm to quantify the degree of fiber alignment occurring in a collagen gel undergoing simulated acupuncture therapy. PLM images were stored as a time series of bitmap image files and fed into a routine developed in MATLAB. This routine provides a continuous index of aligned fiber area by means of binarization of PLM images.

During simulated acupuncture needling, a birefringence pattern emerges in PLM images and grows in size and intensity as needle rotation continues. The birefringence pattern continues to grow until the collagen network fails, at which point the intensity in the image sharply decreases (Fig. 3). Plotting the area of pixels above a certain intensity threshold (see IIB-*v*) against the amount of needle revolutions yields a function that increases exponentially until the point at which the collagen network loses integrity. We define this global maximum in the alignment area vs. needle revolutions curve as the failure point for the collagen sample.

iv. Background Subtraction

Certain conditions, such as increasing collagen concentration, increase the baseline signal in un-needled collagen gels in polarized light images. In order to create a constant criterion for alignment comparison across parameter changes, the mode intensity in the first image in the time series for each sample was taken to be 'background,' as this signal occurs prior to any needle rotation. This background level was subtracted from all proceeding images in the time series, ensuring that all measurements for each collagen sample start at the same initial value and smoothing out day-to-day fluctuations.

v. Determining Intensity Threshold

The degree of fiber alignment in a collagen gel was obtained by calculating the area of the birefringence pattern in the PLM images by way of binarization. Images were subjected to an intensity threshold and the final binary image consists of values of ‘0’ at areas of randomly aligned fibers or fibers aligned perpendicular or parallel to the optical axes, and values of ‘1’ for fibers aligned at angles off the optical axes.

The objective of our threshold routine is to extract the area of the birefringence pattern in PLM data, which we correspond to the area of aligned fibers in the collagen gel. The average intensity of this birefringence pattern in PLM can vary between different parameters, so in order to make comparisons in fiber alignment area across various parameters the threshold value must be determined by geometric criterion rather than intensity.

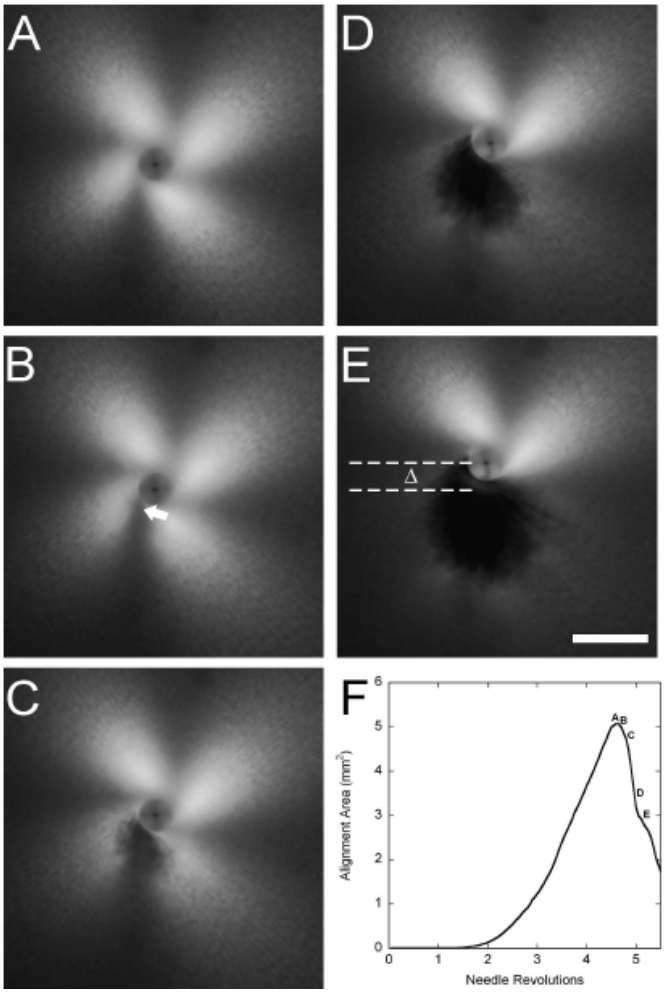

Figure 3 - Winding and failure of collagen gels during *in vitro* acupuncture. (A) The birefringence pattern in PLM images increases in size as needle rotation progresses until gel failure. (B-E) Failure in the gel occurs at the transition point between radially aligned fibers and circumferentially aligned fibers as indicated by the arrow. The tearing in the gel results in decreased area of the birefringence pattern. (F) Quantification of birefringence pattern using an intensity threshold vs. needle revolutions shows that the maximum alignment just prior to gel failure. The points in time correlating to images A-E are marked on the plot. Bar 1mm.

The routine for extracting the boundary of the birefringence pattern using an intensity threshold involves taking a PLM image at set point in the time series prior to gel failure and displaying the corresponding binary images at decreasing threshold intensity values, starting at the maximum intensity represented in the image. As the threshold intensity decreases, the 4-leaf clover birefringence pattern begins to emerge (Fig. 4). The operating threshold value was taken as the intensity value that produced the first complete clover structure in the binary image. This allows us to correlate an intensity threshold value to the geometric shape we are interested in measuring.

All images within the time series are subjected to this final threshold value, and the area of birefringence is calculated and recorded as a function of needle rotation. This threshold routine was performed at the number of needle revolutions across all samples within a certain condition, which was determined by the minimum amount of needle revolutions the gels within that condition could withstand before failure.

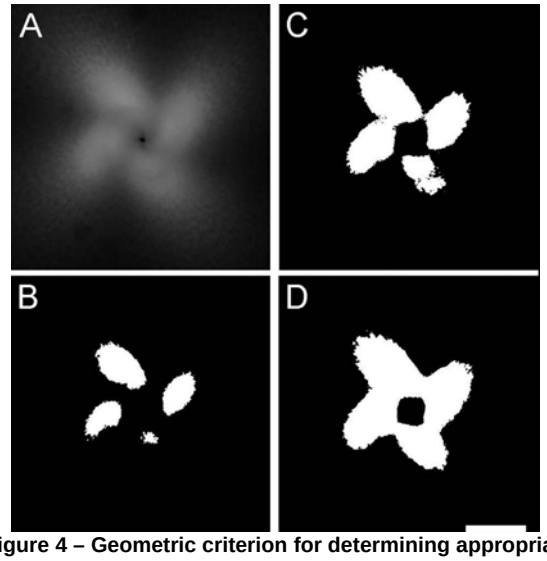

Figure 4 – Geometric criterion for determining appropriate intensity threshold. (A) The threshold is determined at the final frame of the image set. Binary images are sequentially displayed at decreasing threshold values. As the threshold value is decreased, the clover pattern begins to emerge (B, C). The final threshold value is chosen when the complete clover appears in the resulting binary image (D). Bar 1mm.

IIC. Results

i. Quantitative PLM

The quantitative PLM routine described provides a useful tool for a continuous assessment of fiber alignment during simulated acupuncture therapy. We can infer collagen fibers winding around the acupuncture needle by observing the resulting fiber alignment, and our quantitative PLM routine provides us enough sensitivity to document how changes in matrix properties affect the magnitude of the biophysical response.

ii. Image Processing

Quantifying PLM images in our *in vitro* acupuncture model involves calculating the area of birefringence pattern in acquired images, which we equate to the area of aligned fibers. There are many sophisticated image processing techniques available to accomplish this but many of them are computational demanding and overly complicated for our purposes. In order to understand how fiber alignment evolves, data acquisition in our system involves collecting a series of real-time images at 6 frames per second as needle rotation progresses, and the end result is a large amount of images for each experimentation sample (~100 images per gel). Given this large amount of images, a simpler method for quantifying PLM images holds more value than more complicated methods since it allows us to analyze a large amount of data in a more efficient manner.

iii. Background Subtraction

The mean background intensity in PLM images of collagen gels increases with certain parameters, such as collagen concentration. This background shift can be clearly observed in Figure 5A, which shows the histogram of intensity values in collagen gels at various collagen concentrations prior to needle rotation. Since our quantitative algorithm depends on an intensity threshold, we want to ensure that all signal that overcomes the threshold is solely a result of fiber

alignment and not due to this background shift. By subtracting the mean intensity value in images of un-needled collagen gels, we can shift the intensity mean towards '0' and normalize background intensity across collagen concentration (see Figure 5B).

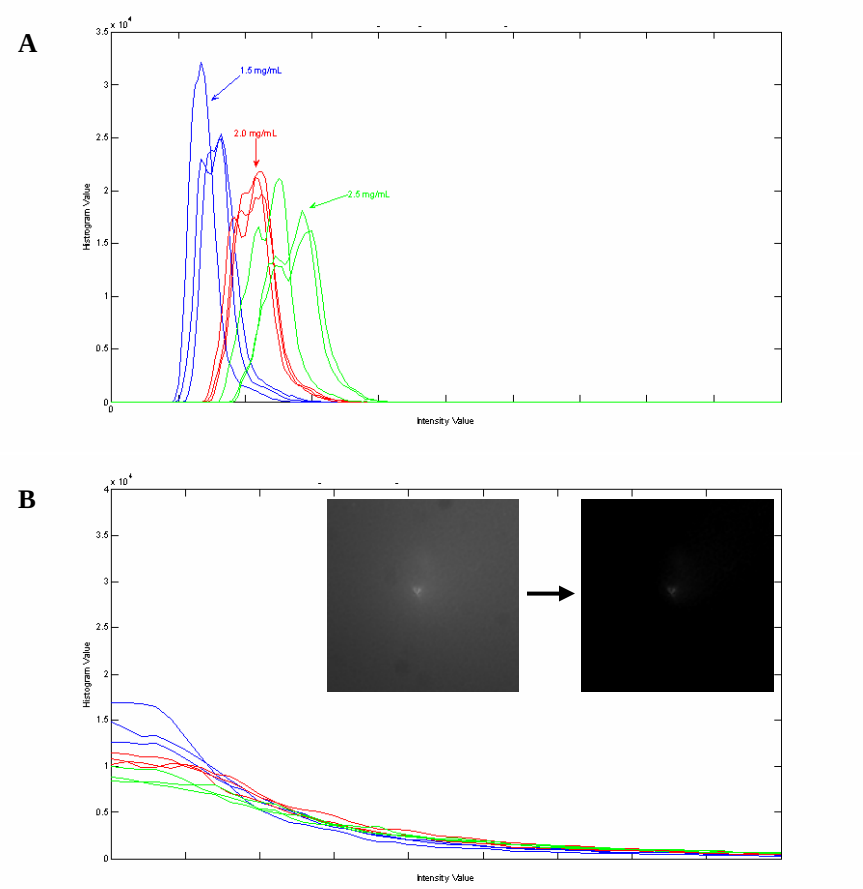

Figure 5 – Mean background intensity in PLM images of un-needled collagen gels in shifts with changes in collagen concentration. (A) Histogram representation of intensity values shows an increase in the mean intensity value in PLM images as collagen concentration increases. Collagen concentrations shown are 1.5 mg/mL (blue), 2.0 mg/mL (red), and 2.5 mg/mL (green). (B) By taking the mode intensity value in un-needled gel images and subtracting this from all corresponding images, we can normalize the background intensity across collagen concentration. This subtraction routine eliminates the contribution of this background shift on quantitative data extracted by the threshold. Inset: PLM image of un-needled collagen gel before (left) and after (right) background subtraction routine.

iv. Determining Intensity Threshold

One of the simplest methods for calculating the area of a region of interest is to subject an image to an intensity threshold and extracting the resulting binary image. By selecting an intensity value that correlates to the boundary of the birefringence pattern in PLM images, the resulting binary image will contain the area of aligned fibers. The average intensity within the birefringence pattern can vary significantly over day-to-day experiments as well as across gel conditions such as collagen concentration. As a consequence, the intensity value that accurately describes the boundary of the birefringence pattern also exhibits this variation (see Figure 6). In order to account for this variation during quantification, the algorithm utilizes a geometric criterion for determining the intensity threshold value for each experiment individually. By identifying which intensity value accurately describes the boundary of the birefringence pattern for each individual gel we extract the exact area of aligned fibers without the inherent variations within our system. This geometric criterion for intensity threshold selection minimizes the contribution of factors other than fiber alignment in our quantitative data, reducing the error in our measurements (see Figure 7).

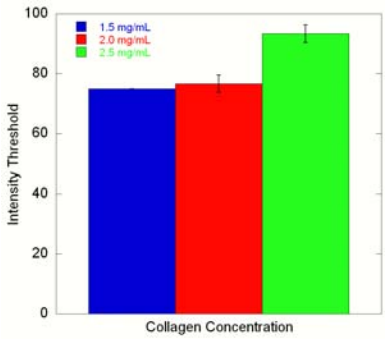

Figure 6 – Example of the variation in intensity threshold across collagen concentration. The intensity value that accurately describes the boundary of the birefringence pattern in PLM images increases along with collagen concentration. Our image processing algorithm accommodates for this by determining the observing the intensity threshold that best describes the birefringence pattern boundary individually for each experiment.

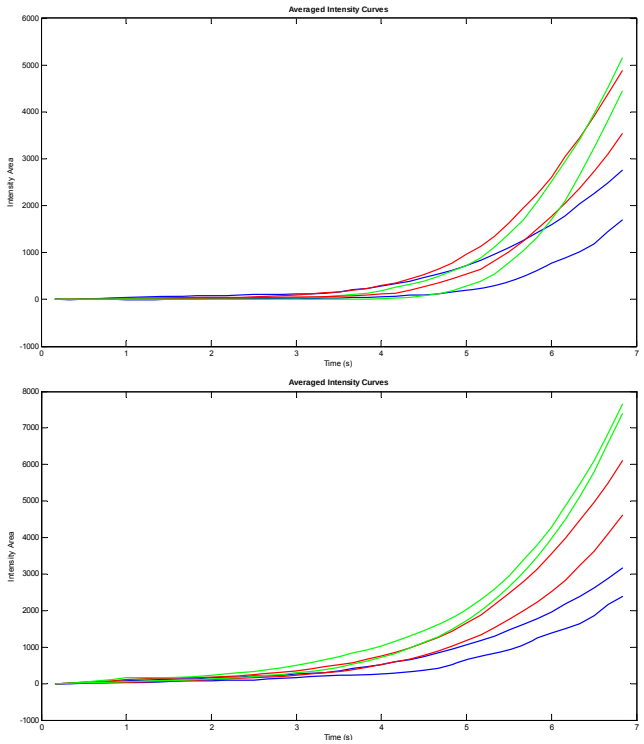

Figure 7 – Area of birefringence pattern during needle rotation as determined by an intensity threshold. Gels are either fixed (dashed) or left untreated (solid) and prepared at three different collagen concentrations: 1.5 mg/mL (blue), 2.0 mg/mL (red), and 2.5 mg/mL (green). (A) Quantification using a signal intensity threshold across all parameters results in a large amount of error with no discernable trend. (B) Using a geometric criterion for determining the intensity threshold for each gel individually reduces the error in our measurements, allowing us to detect trends in fiber alignment across gel parameters such as collagen concentration and fiber cross-linking.

III. Objective 2 – Directly observe the biophysical response of fibrous protein networks during simulated acupuncture therapy.

IIIA. Introduction

It has been shown that during acupuncture therapy, fibers in the loose connective tissue coupled and wind around the acupuncture needle as it is rotated[2]. Tissue deformation incurred during acupuncture therapy has been observed in previous studies by ultrasound scanning and histology of the subcutaneous connective tissue[5]. It has been hypothesized that fibers winding around the needle functions as the biophysical mechanism for this behavior, however this hypothesis has not been able to be directly observed in previous research due to the limitations inherent with *in vivo* and *ex vivo* research.

We believe that our *in vitro* assay of acupuncture therapy provides an avenue to directly observe the biophysical behavior of fibers in an extracellular matrix (ECM) winding around the rotating needle. Fiber winding and the ensuing tissue deformation is a vital component to the theory of connective tissue involvement in acupuncture's therapeutic benefits. The major components of loose connective tissue are networks of fibrous extracellular matrix (ECM) and interconnected fibroblasts (ECM). These fibroblasts respond to mechanical signals in the connective tissue, such as tissue stretch, with dynamic changes in the cytoskeleton and cell shape[11]. During acupuncture therapy performed on connective tissue explants, similar changes in cell morphology occur as the displacement of ECM fibers during winding of the tissue causes a force on focal contacts in the cell[6]. Biomechanical signals can cause significant biochemical processes in a cell, such as the regulation of mechano-sensitve genes[13]. It is theorized that the therapeutic effects that result from acupuncture treatment could arise from the cell response to this unique biomechanical signaling environment[3].

Biochemical processes that may contribute to the therapeutic mechanism of acupuncture could result from the tissue displacement ensuing from fiber winding. Previous research endeavors lack the ability to directly observe the tissue response during fiber winding and are deficient in any

quantitative description of the biophysical behavior arising from needle rotation. Using our *in vitro* system, we can accomplish both of these tasks by suspending displacement indicators within our *in vitro* tissue models, such as polystyrene beads, and tracking the bead movement as they displace with the tissue throughout needle rotation. For method development purposes, we have selected to use fibrin gels as our connective tissue model. Fibrin gels generate more displacement during needling and can withstand more needle revolutions before failing than collagen, providing the ideal medium for developing the displacement tracking algorithm. Though fibrin is a much less abundant component of connective tissue, it exhibits biophysical behavior similar to other fibrillar protein gels such as collagen.

IIIB. Methods

i. Fibrin Gel Preparation

A stock solution of fibrinogen dissolved in 1x phosphate-buffered saline (PBS) was diluted in 10x MEM, 1x PBS with calcium, and a 3 unit/mg solution of thrombin in 1x PBS to a final concentration of 3.0 mg/mL fibrinogen. A 35 mm Petri dish was prepared with an outer ring (polydimethylsiloxane *PDMS*, OD 35 mm, ID 25.4 mm) and an inner ring (porous polyethylene *PPE*, OD 25.4 mm, ID 15.9 mm) to provide a fixed boundary for the fibrin gel (Fig 8). The 3.0 mg/mL fibrinogen-thrombin solution was seeded with 100-125 μm polystyrene beads, plated into the void of the dish assembly, and incubated at 37° for four hours to ensure complete fibril formation. In certain cases, the structure of fibrin gels was altered by exposing the matrix to 2% formalin solution for 10 minutes to asses the effect of fiber cross-linking on gel displacement during acupuncture needling.

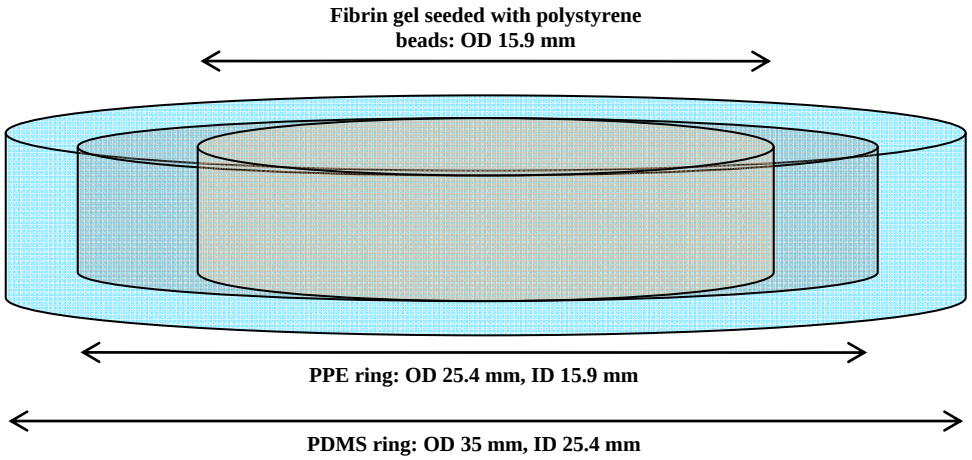

Figure 8 – Preparation of fibrin gels seeded with polystyrene beads. Fibrin gels are incubated in this assembly for 4 hours and are then subjected to simulated acupuncture therapy.

ii. Simulated Acupuncture Therapy

In vitro acupuncture therapy was performed in a similar fashion as mentioned previously. Three PDMS rings (OD 35 mm, ID 25.4 mm) where stacked in a glass-bottom MatTek dish, with the PPE ring contained the fibrin gel situated in the middle ring of the stack (Fig 9), and the void of the PDMS rings were filled with a reservoir of 1x PBS as to completely submerge the fibrin sample. A stainless steel acupuncture needle was inserted through the fibrin gel and needle rotation was performed by a computer-controlled motor at 0.3 rev/second for 10 needle revolutions. A fiber-optic ring light was attached to the motor to provide a light source, and images were captured using a USB CCD camera at 6 frames per second. All imaging was performed by bright-field microscopy, with a single polarizer inserted into the optic train to improve the contrast between beads and background in captured images.

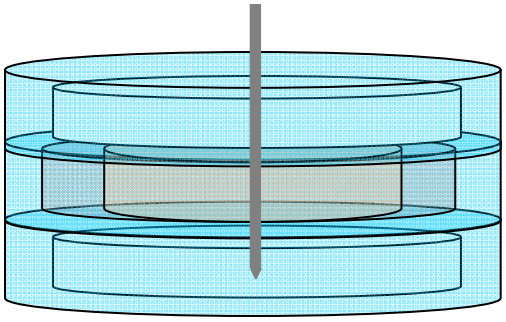

Figure 9 - Fibrin gel assembly during simulated acupuncture therapy. The gel seeded with polystyrene beads was situated between two PDMS rings and submersed in saline. The needle was interested through the entire length of the gel prior to needle rotation.

iii. Image Processing

Data was collected as a series of images to chronologically document the displacement of seeded beads in the fibrin network as acupuncture needling progresses. The background intensity of the acquired bright-field images prior to needling consists of a constant intensity level, but as fiber alignment occurs during needle rotation the background intensity begins to vary throughout the image. This varying background consists of maximum intensity at the needle insertion point and decreasing outward radially. In order to properly threshold out the shapes of the beads for proper displacement tracking, the varying background was negated by performing a morphological opening routine on raw data images.

Morphological opening on the raw images was performed using a disk structuring element on each individual frame in the chronological series of images. This routine, consisting of an image erosion and dilation, effectively removes the beads from the image foreground and isolates the varying background. This background is then subtracted from the image, extracting the foreground populated solely by the beads.

Binary images are created by subjecting the images to an intensity threshold, the value of which is determined by observing the intensity value at the boundary of the bead edges. A morphological bridge operation is performed to ensure that all beads form a complete circle, and then the boundary of the bead edges are recognized and the centroid of each bead is recorded as the bead's position.

iv. Bead Tracking

The image processing routine described above produces a matrix of bead positions for each individual frame in the chronological series of images. The individual displacement vector for each bead as needle rotation progresses was obtained by feeding the position matrices and raw data images into a routine developed in MATLAB.

The initial bead positions are displayed on the first frame of the image and positions that do not correctly correspond to a bead are manually selected and removed from the position matrix, removing any false positions produced by the image processing algorithm. For each bead within an individual frame in the chronological series, the Euclidean distance between the bead's position and all positions in the next frame is calculated. The minimum distance calculated in this fashion is assumed to be the distance traveled by that bead, and the corresponding position is recorded as the bead's next position in time.

IIIC. Results

Simulated acupuncture therapy is performed by inserting a needle through a fibrin gel seeded with polystyrene beads and rotating. As the needle rotates, suspended beads began to displace both radially and circumferentially as the tissue deforms. In the regions distal from the needle, the primary direction of bead displacement is radial towards the needle. Once the beads begin to approach the needle, their displacement behavior shifts from radial to circumferential and the beads eventually end at a trajectory that circumscribes the needle as it rotates.

Rotation of the acupuncture needle causes a coupling and winding for ECM fibers around the needle, causing surrounding tissue to displace. These fibers wrap around the needle, straining the fibers and inducing radial alignment in the surrounding areas[10]. We see a similar pattern in displacing beads, demonstrating that our beads travel along with the tissue during simulated acupuncture therapy.

Bright-field microscopy was used to capture images of the beads displacing during simulated acupuncture therapy, and the algorithm described allows us to track the individual trajectory of each bead during this motion (Fig 10). Results from three different fibrin gels over several days showed good consistency, with radial displacement of beads averaging at 1.41 ± 0.04 mm over 8 needle revolutions. Error during bead tracking was minimal, and generally limited to breakdown in identifying centroid positions of beads clustered together. For example, two beads clustered together would be tracked by our algorithm as a signal displacement vector with the position value alternating between the centroid of each bead. This error results in the ‘zig-zag’ trajectories that can be seen in Figure 10, and the influence of this error appears to be negligible.

`

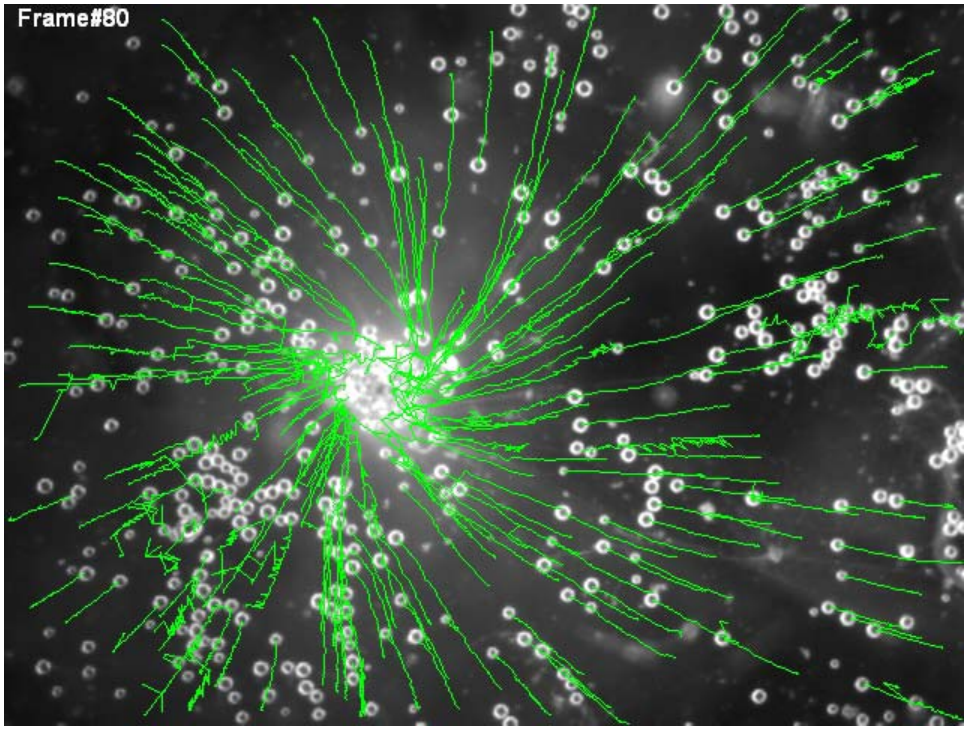

Figures 10 – Trajectories of displacing beads within a fibrin gel undergoing simulated acupuncture needling are displayed in green. The beads displace primarily in the radial direction throughout the gel and transition into a circumferential displacement as they approach the needle.

IV. Discussion

While performing acupuncture the therapist inserts fine needles at specific acupuncture points depending on the ailment to be treated and performs a complex range of needle manipulations, the most basic of which involves needle rotation. Acupuncture therapy involves using the phenomenon of *de qi*, or needle grasp, as an indicator of appropriate needle manipulation. Despite the use of acupuncture as an alternative medical practice, the mechanism of needle grasp and its relation with ensuing therapeutic benefits have remained largely unknown. Analysis of tissue remnants present on acupuncture needles after removal from patients have shown the presence of connective tissue proteins, specifically collagen and elastin[12], hinting that subcutaneous connective tissue may be involved in needle grasp. Extensive research by Langevin et al. suggests that needle grasp occurs as collagen fibers in the subcutaneous connective tissue couple and wind around the rotating acupuncture needle, generating stress and strain fields in the surrounding tissue[7]. These mechanical signals have been observed to cause considerable cytoskeletal changes in fibroblasts populating connective tissue, suggesting that this tissue deformation may result in numerous downstream effects, including gene expression and neuromodulation[2, 3]. This strong volume of evidence further suggests that mechanotransduction within the subcutaneous connective tissue may play a significant role in the mechanism of acupuncture therapy.

In vivo and *ex vivo* experiments have proven vital for uncovering this evidence of connective tissue involvement during acupuncture therapy. However the nature of these systems have not permitted direct observation of the suggested biophysical behavior of collagen fibers to acupuncture needle rotation and has left unanswered questions about the properties of connective tissue that permit this unique response. These limitations provide the motivation for the development of *in vitro* tools for analyzing the biophysical response of tissue to acupuncture therapy in a simplified, controlled setting. Using these tools allow us to break down the hypothesis of connective tissue involvement during acupuncture therapy to the most basic level and determine if the biophysics observed support existing theories.

When a needle is inserted into a patient, contact is made with several types of tissue including skin (epidermis and dermis), subcutaneous fat, loose connective tissue, and muscle. However when needle rotation commences, only loose connective tissue couples and winds around the needle creating the characteristic 'whorl' pattern previously observed[4]. The properties of this tissue that generate this unique response remain unknown and identifying these parameters *in vivo* is complicated by variation inherent to biological tissues. Studying the response of tissue models to needle rotation in our *in vitro* system allows us to control the parameters of our tissue models in a simplified setting without this complex variation. By observing parameters that increase or decrease the tissue's ability to respond to simulated acupuncture therapy, we can begin to speculate about the properties that permit the exclusive involvement of subcutaneous connective tissue during treatment.

The suggested biophysical mechanism for loose connective tissue involvement in acupuncture therapy is collagen fibers in the extracellular matrix coupling and winding around the rotating needle. We have chosen to use acellular type I collagen gels as our model for connective tissue and our objective is to observe the effect of different gel parameters (collagen concentration, cross-linking, tissue thickness, needle insertion depth, etc.) on the tissue's ability to respond to needle rotation. In order to make comparisons across conditions, we need a quantitative index that reliably describes the magnitude of tissue response. We can extract such an index using polarized light microscopy (PLM). Connective tissue has been observed to transition from a random state to a much higher ordered state as fibers in the tissue align due to the strain produced by needle rotation[4]. Capturing PLM images during simulated acupuncture therapy allows us to easily observe this increasing anisotropy in collagen gels and calculating the area of birefringence enables us to gauge the magnitude of fiber alignment quantitatively.

Using our *in vitro* system we can begin to investigate the role of matrix mechanostructural properties in the tissue's ability to respond to acupuncture therapy. For example, we observe that increased fiber alignment in gels with a higher concentration of collagen (Fig 11). Similarly, increased gel stiffness by means of exposure to a cross-linking agent was shown to decrease the

fiber alignment generated by acupuncture needle rotation (Fig 12). These two simple observations demonstrate how our system can be used to hypothesize as to why connective tissue selectively responds to needle rotation. The majority of extracellular matrix in loose connective tissue is comprised of collagen at high concentrations and this tissue is much more compliant then adjacent tissues such as muscle and skin. Our *in vitro* observations suggest that properties such as these allow connective tissue to respond more readily to acupuncture needling while other tissues do not.

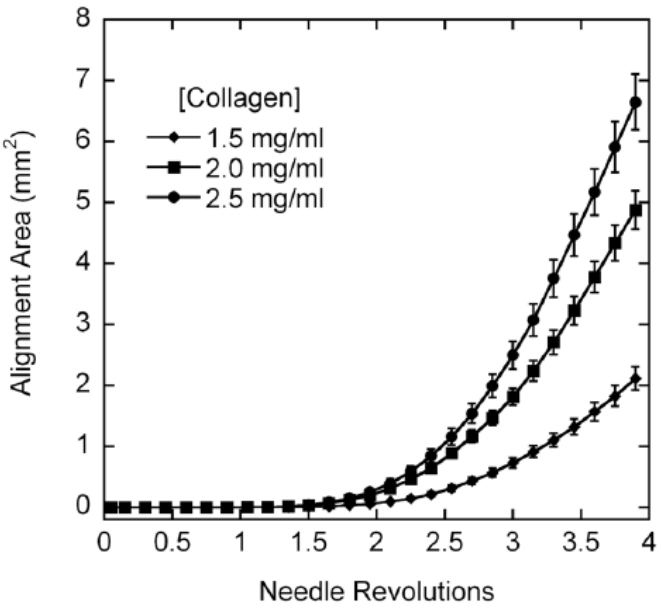

Figure 11 – Area of aligned fibers across collagen concentration (average ± standard error). Using quantitative PLM we are able to observe a significant increase in the rate of fiber alignment as collagen concentration increases.

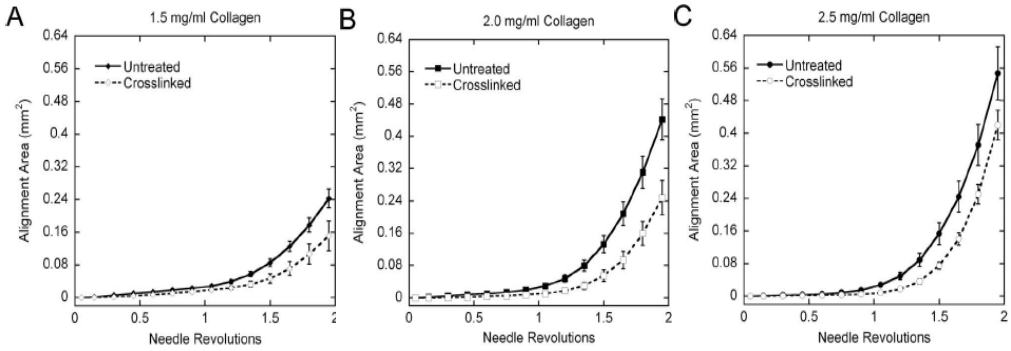

Figure 12 – Increasing the degree of fiber cross-linking significantly affects the progression of fiber alignment as needle rotation progresses (average ± standard error). Collagen exposed to 10% formalin aligned at a slower rate than untreated collagen at all concentrations observed.

We can directly observe the tissue's response to acupuncture needle rotation by observing the displacement of suspended polystyrene beads within our connective tissue models. Once the needle is inserted through the tissue and begins to rotate, fibers couple and wind around the needle, straining the surrounding tissue as inter-fibril connections generate a displacement field. This displacement field originates very close to the needle surface but increases radially outward the more the needle is rotated, pulling increasing amounts of tissue in towards the needle. Displacement resulting from needle rotation can be described as a gradient with displacement decreasing with radial distance away from the needle (Fig 13). The strain resulting from the displacement gradient results in the fiber alignment observed under polarized light microscopy, demonstrating the relationship between our quantitative index of tissue response in Section II and observation of bead displacement in Section III. We observe a similar dependence on matrix properties with both bead displacement and fiber alignment (Fig 14).

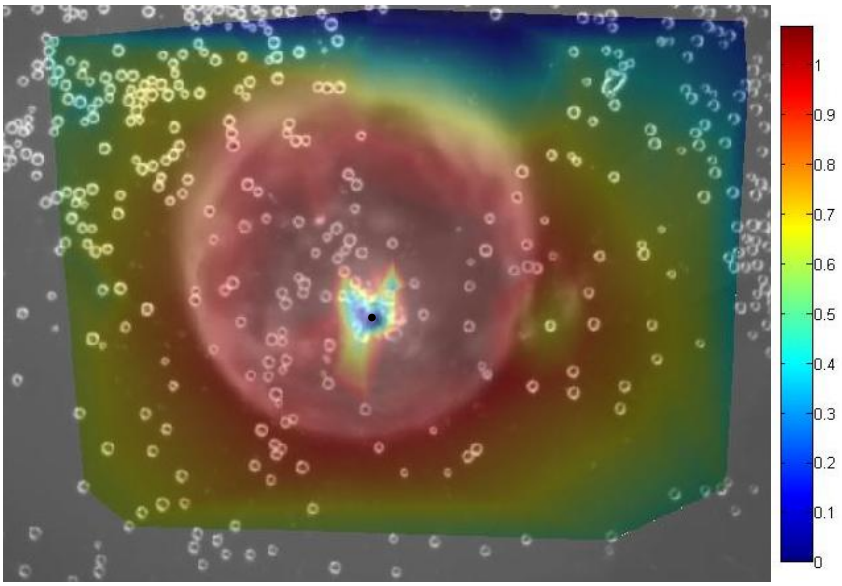

Figure 13 – Polystyrene beads with a fibrin gel displacing after 4 needle revolutions. Magnitude of radial displacement vector (in mm) for each bead is displayed. The acupuncture needle is marked with a black dot. We observe greater displacement in beads closer in proximity to the needle. As beads approach the region of circumferentially aligned fibers wound around the needle, the radial displacement drops to 0 and the beads enter a primarily circumferential motion.

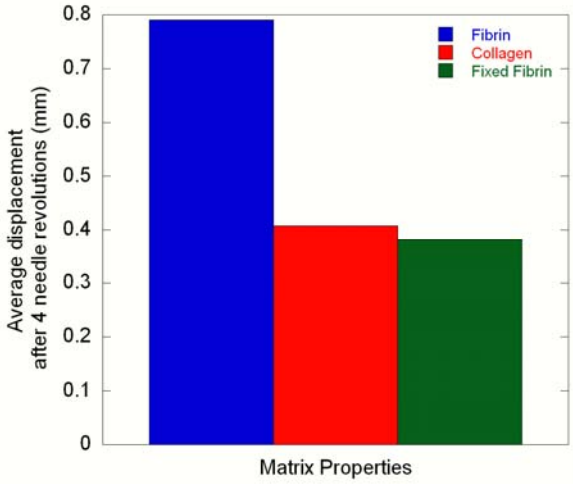

Figure 14 – Dependence of bead displacement on mechanostructural properties of the matrix. After 4 needle revolutions, we observe greater average bead displacement in fibrin gels than collagen gels. We also observe a decrease in average bead displacement when with an increase in inter-fiber connections by exposing the fibrin matrix to a cross-linking agent. Note a similar relationship between matrix mechanostructural properties and fiber alignment (see Section II).

The biophysical behavior observed by tracking bead displacement during acupuncture needle rotation provides insight towards the mechanism of connective tissue involvement in acupuncture therapy. Subcutaneous connective tissue exists as a continuous plane in the body through inter-fibril and cell-cell connections. When an interested needle begins to rotate, the fiber winding displaces surrounding tissue inward towards the needle. The region of displacing tissue increases as needle rotation continues, suggesting that mechanical signals generated could travel into distal regions away from the needle along the continuous plane of connective tissue. The complex therapeutic benefits provided by acupuncture therapy could be a result of both local and distal affects of needle rotation ranging from modification of gene expression in subcutaneous fibroblasts to modulation of sensory neurons present within the connective tissue.

The tools developed for our *in vitro* system of acupuncture therapy have demonstrated consistent results, agree with published research from *in vivo* and *ex vivo* studies, and support current theories of the role of connective tissue involvement in the mechanism of acupuncture therapy. However use of these tools has been limited to proof-of-principal models for method development purposes. Further complication of our tissue models will allows us to further investigate the roles of tissue properties on acupuncture therapy. These complications can include additional constituents of connective tissue such as cellular populations and other matrix components such as proteoglycans. The quantitative nature of our *in vitro* systems will allow further characterization of the roles of various tissue properties on the connective tissue's ability to respond to acupuncture therapy. This information, in conjunction with further *in vivo* and *ex vivo* studies, will hopefully lead investigators further down the path to discovering the elusive mechanism of acupuncture therapy.

V. Conclusion

We have developed an *in vitro* platform for studying the mechanotransduction in connective tissue generated by acupuncture therapy in a highly controlled quantitative setting. This setting allows us to control parameters in our tissue models and use quantitative tools to assess the role of these properties on the tissue's ability to respond to acupuncture therapy. With this system we have already been able to make observations that suggest the specific mechanostructural properties of loose connective tissue allow its unique biophysical response to acupuncture needling. This thesis outlines the computational tools developed for extraction of quantitative data from *in vitro* experiments. Data from these tools have demonstrated precision by consistent results among various experiments, as well as accuracy with results that agree with previous published research. It is our belief that our *in vitro* system will prove itself as a valuable asset in studying the role of connective tissue involvement during acupuncture therapy, and provide investigators with further insight while attempting to undercover the mechanism of acupuncture therapy.

VI. References:

1. Acupuncture. NIH Consensus Statement Online 1997 Nov3-5; 15(5):1-34

2. Langevin HM, Churchill DL, Fox JR, Badger GJ, Garra BS, Krag MH: Biomechanical response to acupuncture needling in humans. *J Appl Physiol* 2001, 91(6):2471-2478.

3. Langevin HM, Churchill DL, Cipolla MJ: Mechanical signaling through connective tissue: a mechanism for the therapeutic effect of acupuncture. *Faseb J* 2001, 15(12):2275-2282.

4. Langevin HM, Churchill DL, Wu J, Badger GJ, Yandow JA, Fox JR, Krag MH: Evidence of connective tissue involvement in acupuncture. *Faseb J* 2002, 16(8):872-874.

5. Langevin HM, Konofagou EE, Badger GJ, Churchill DL, Fox JR, Ophir J, Garra BS: Tissue displacements during acupuncture using ultrasound elastography techniques. *Ultrasound Med Biol* 2004, 30(9):1173-1183.

6. Langevin HM, Bouffard NA, Badger GJ, Churchill DL, Howe AK: Sub-cutaneous tissue fibroblast cytoskeletal remodeling induced by acupuncture: evidence for a mechanotransduction-based mechanism. *J Cell Physiol* 2006, 207(3):767-774.

7. Langevin HM, Bouffard NA, Churchill DL, Badger GJ: Connective tissue fibroblast response to acupuncture: dose-dependent effect of bidirectional needle rotation. *J Altern Complement Med* 2007, 13(3):355-360.

8. Langevin HM, Yandow JA: Relationship of acupuncture points and meridians to connective tissue planes. *Anat Rec* 2002, 269(6):257-265.

9. Tower T, Tranquillo R. Alignment maps of tissues: I. Microscopic elliptical polarimetry. Biophysical Journal 2001, 18: 2954-2963.

10. Julias M, Edgar LT, Buettner H, Shreiber D. An in vitro assay of collagen fiber alignment by acupuncture needle rotation. *BioMed Eng Online* 2008 7:19.

11. Langevin HM, Bouffard N, Badger G, Iatridis J, Howe A: Dynamic fibroblast cytoskeletal response to subcutaneous tissue stretch ex vivo and in vivo. *Am J Phyiol Cell Physiol* 2005, 288 C747-C756.

12. Kimura M, Tohya K, Kuroiwa K, Oda H, Gorawski EC, Hua ZX, Toda S, Ohnishi M, and Noguchi E. Electron microscopical and immunohistochemical studies on the induction of 'qi' employing needling manipulation. *Am J Chin Med* 20: 25–35, 1992.

13. Banes, A. J., Tsuzaki, M., Yamamoto, J., Fischer, T., Brigman, B., Brown, T., and Miller, M. (1995) Mechanoreception at the cellular level: the detection, interpretation and diversity of responses to mechanical signals. *Biochem. Cell Biol.* 73**,** 349–365.